Available online at www.sciencedirect.com

ScienceDirect

Physics Procedia 12 (2011) 404–410

Physics Procedia

LiM 2011

Plasma Monitoring during Laser Material Processing

David Diego-Vallejo[a,b], David Ashkenasi[c,]*, Gerd Illing[c], Hans Joachim Eichler[a]

[a]*Technische Universität Berlin, Institut für Optik und Atomare Physik, Straße des 17. Juni 135, 10623 Berlin, Germany*
[b]*Instituto Politécnico Nacional, U.P. Adolfo López Mateos - Zacatenco, Mexico City, 07738, Mexico*
[c]*Laser- und Medizin-Technologie Berlin GmbH, Fabeckstr. 60-62, 14195 Berlin, Germany*

Abstract

Spectroscopic analysis of the emitted plasma during laser machining can provide valuable information on the relevant material reaction channels and removal rates. The aim of the study is the improvement of the laser micro machining results by means of laser-induced breakdown spectroscopy. Two applications in online monitoring and control are demonstrated: 1. optimization of laser beam focus repositioning on the work piece during trepanning; 2. depth control in selective thin film removal in multi layer systems.

Keywords: Laser machining; trepanning; LIBS; processing monitoring; thin-layer monitoring

1. Introduction

Laser-Induced Breakdown Spectroscopy (LIBS) is a technique widely used for qualitative and quantitative chemical analysis due to its intrinsic advantages like in-situ and real-time analysis, little or no sample preparation, multiple element identification capability and almost non-invasive measurement owing to the minimum amount of material ablated [1]. Moreover, LIBS has proved to be a successful tool for on-line material identification and sorting [2,3], controlled surface cleaning in archeological sciences [4,5], multi-layer removal monitoring [6] and thickness or depth measurements [7,8].

Laser machining can benefit from this technique given that during material processing, plasma emission takes place. The amount of ablated material can be estimated based on the intensity of the emission lines and further analysis can lead to an insight of the instant characteristics or quality of the machining. Furthermore, a strategy applied to improve laser processing of brittle materials is the use of trepanning strategies. By this mean it is possible to increase the quality of the edges in glass machining and even to control the taper structure [9]. A trepanning system is used in this work to observe its influence in plasma emission.

The objective of this study is to investigate the influence of processing parameters in the emitted plasma with the aim of finding useful relationships to be applied as monitoring signal during machining of different materials. A

* Corresponding author. Tel.: +49-30-84492377; Fax: +49-30-84492399.
E-mail address: d.ashkenasi@lmtb.de.

doi:10.1016/j.phpro.2011.03.150

multi-layer material for photovoltaic applications is used to evaluate the selective thin-film removal capability of the system.

2. Experimental

2.1. Instrumentation

The experimental setup is sketched in Figure 1. Two different diode-pumped solid-state laser systems are used for the experiments, each one working at a different pulse-duration regime: A Q-switched Nd:YVO_4 laser system with an amplifier stage (IB-Laser, Germany) generating laser pulses at a pulse width ca. 20 ns at 1064 and 532 ns. A picosecond Nd:YVO_4 laser system (Super-Rapid, Lumera, Germany) with a pulse width of 10 ps at 1064 nm and 7 ps at 532 nm. The samples are placed on an XYZ positioning stage. A LMTB mechanical laser trepanning system focuses and rotates the laser beam on the work-piece. The focal length in the trepanning system used for this study is 50 mm. The rotation speed used for all the experiments is 1000 rpm, more details can be found elsewhere [9].

A 0.75x microscope objective focuses the spectroscopic signal into an optical fiber connected to an Ocean Optics USB2000+UV-VIS spectrometer with a resolution of 0.316 nm. The analyzed spectral band is 350 to 800 nm. An on-axis acquisition configuration is used. Integration time is set to 100 ms for all experiments except for the thin-film removal monitoring where the integration time was doubled to 200 ms. In the experiments using 532 nm laser pulses, a notch filter for the same wavelength is introduced to suppress the laser reflection during recording. All experiments are conducted at atmospheric pressure.

For the studies of the influence of the trepanning optics, wavelength and pulse width, glass processing and focus monitoring the following parameters are used: For nanosecond investigations (in both infrared and green) the energy per pulses is 0.45 mJ at a repetition rate of 20 kHz and for picosecond experiments 0.18 mJ per pulse at 50 kHz. For the studies on thin layer removal, the energy per pulse is set to 4 µJ at 10 kHz. XY motion speed equals 20 mm/s. The trepanning optics can de replaced for comparison by a best-form quartz lens with a focal length of 100 mm.

The spectroscopic signal is acquired during material processing. In other words, processing quality and efficiency is the main overall goal of the investigations. This study discusses the identification of possible correlations between “optimal” processing parameters and spectral data, acquired during the online monitoring of the plasma.

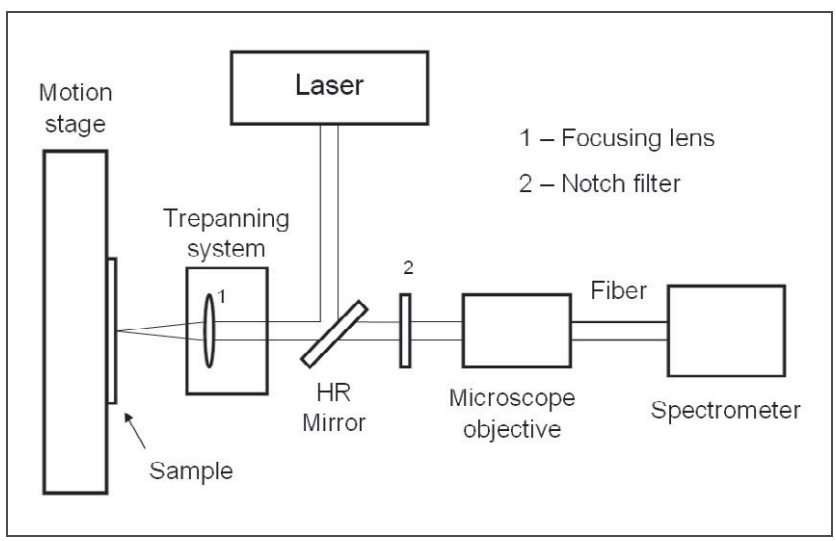

Figure 1. Schematic of the setup for acquisition of plasma signal during laser processing.

2.2. Samples

Ceramic samples like AlN, Al_2O_3 and SiC as well as technical glasses like quartz, sapphire, 1737 (Corning), AF45, BK7, borofloat, D263 and soda-lime (Optiwhite) are studied. As references for spectroscopic elemental identification, aluminum (99.999% purity), molybdenum (99.9% purity) and a silicon wafer are used. The solar cell sample used to evaluate the feasibility of selective removal consists of 3 layers, which are, from the outermost to the innermost, ZnO (ca. 2 µm), CIS (Copper-Indium Selenide, 2 µm) and Mo (0.5 µm). These thin film systems are used in photovoltaic applications.

3. Results and Discussion

When a mechanical laser trepanning system is used during machining, the plasma signal is enhanced considerably as observed in Figure 2, improving the signal-to-noise ratio (SNR) up to sevenfold compare data gathered without using it, due to the increased amount of ablated material per time unit produced.

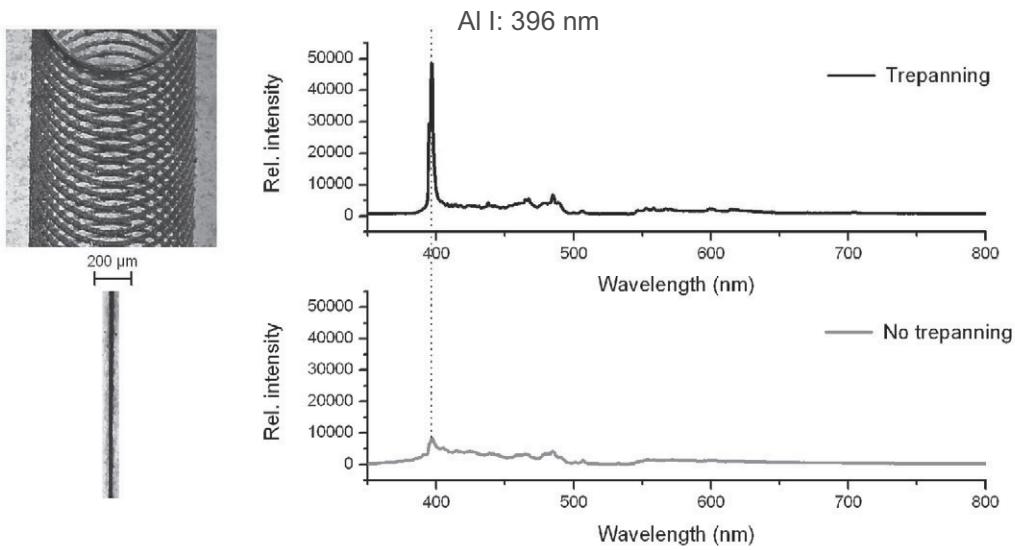

Figure 2. Results on AlN ceramic processing with 532 nm laser radiation and emission spectra acquired with and without the use of a trepanning optics because the emission region is larger.

3.1. Influence of wavelength and pulse width

The influence of different laser wavelengths and pulse widths is shown in Figure 3 for AlN ceramics and borofloat glass. For ceramic AlN and Al_2O_3, for sapphire and pure aluminium, the strongest peak is registered at 396.15 nm, which is identified as an (excited) Al I emission line. Several other peaks can be identified between 400 and 800 nm mainly Al II peaks. However also a N II emission line is observed at 500.27 nm.

The plasma spectra do not differ significantly while shifting the machining laser wavelength from 1064 to 532 nm at 20 ns pulse width. The neutral Al I line becomes more dominating and the background pedestal is reduced, the latter being an effect of decreased thermal emission. The resemblance in the plasma spectra is even more remarkable in the case, where at 532 nm the pulse width is reduced to 7 ps.

In the case of borofloat glass, the highest intensity is observed for double ionized silicon at 589.88 nm but also barium, aluminium and boron lines are identified. Unlike with the results of the Al-based materials, borofloat glass and the barium containing glass samples (BK7, 1737 and AF45) present a slightly different shape in the spectra generated during machining at 532 nm with pulse widths of 20 ns and 7 ps, but the dominant lines remain.

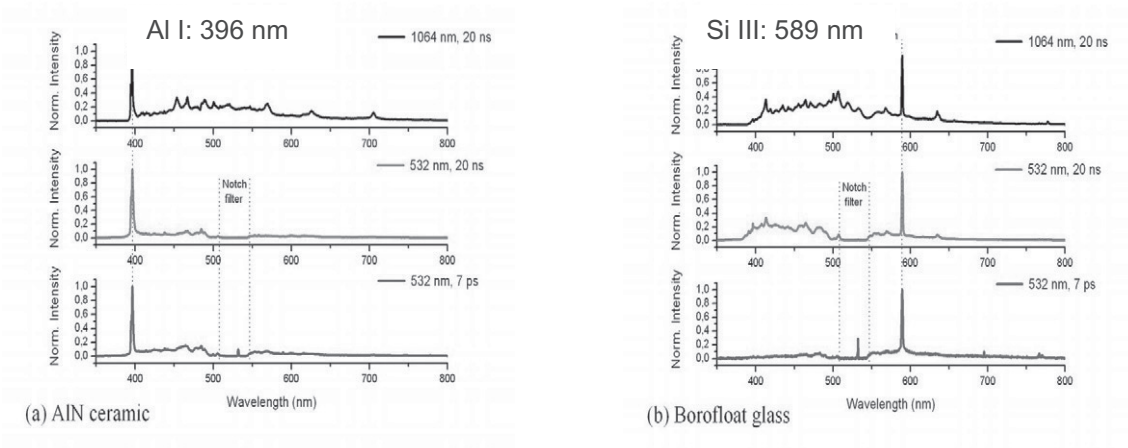

Figure 3. Laser induced plasma spectra during laser processing of a) AlN ceramics and b) borofloat glass at different wavelengths and pulse width. Top: wavelength = 1064 nm and pulse width = 20 ns, middle: wavelength = 532 nm and pulse width = 20 ns, bottom: wavelength = 532 nm and pulse width = 7 ps. The relative intensity was normalized based on the neutral Al line at 396.15 nm for a) and double ionized silicon at 589.88 nm for b).

3.2. Glass type monitoring

Different glass samples are processed with picosecond pulses at 532 nm. The resulting plasma emission spectra obtained for four different glass types, fused silica quartz, Schott display glass AF45, Schott optical glass BK7, and Corning alumina-glass 1737) are depicted in Figure 4.

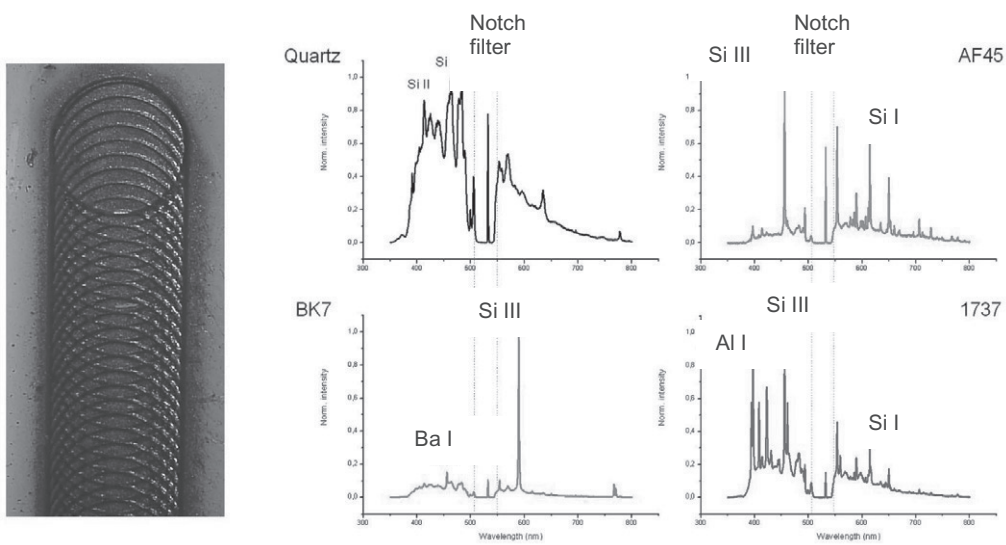

Figure 4. Example of trepanning machining on borofloat glass and spectra of different glass samples. Laser machining was performed with a wavelength of 532 nm and a pulse duration of 7 ps.

The major constituent in the glass samples of this study is silica. However, the spectra show that glass identification or sorting can be achieved based on the intensity of the emission lines of other concomitants, such as Ba or Al. For example, AF45 and 1737 glass are characterized by a similar elemental constitution (SiO_2>50%, Al_2O_3~11%, B_2O_3~7-14% and BaO~5-22%). Both glasses demonstrate, however, fairly different line spectra. While the peak Al I at 396.15 nm is observed to be most dominant for the glass 1737, the identical line is hardly visible in the case of glass AF45. In addition, the line emission around 600 nm in BK7, identified as a transition in double ionized Si III, is quite outstanding compared to the other glass types. On the other hand, the other strong Si III lines near 460 nm, observed for quartz, AF45 and 1737 glass, is not unambiguously identifiable in BK7. These significant differences in the spectra depending on the type of glass is not observed for the samples with (only) Al metal constituents, such as 99.99% Al metal, ceramic Al_2O_3 and AlN, and sapphire. Here, the plasma analysis yields the identical Al I and Al II emission lines with similar intensities. The reason for this observation is unclear. Perhaps collisions between the different metal-like atoms and ions in the laser-induced plasma from the glass samples yield different emission conditions depending strongly on the elemental constitution. Further investigations are planed to follow up on this hypothesis.

3.3. Focus positioning monitoring

Focusing distance is changed in controlled steps during processing and the spectroscopic signal is acquired simultaneously in order to determine possible correlations.

The strongest emission line in the spectrum of each analyzed material is monitored for different focusing distances and the result is displayed in Figure 5, showing that the maximum intensity is reached near the on-focus distance. This effect can be used to implement an adjustment strategy to automatically locate the best focusing conditions prior and during processing.

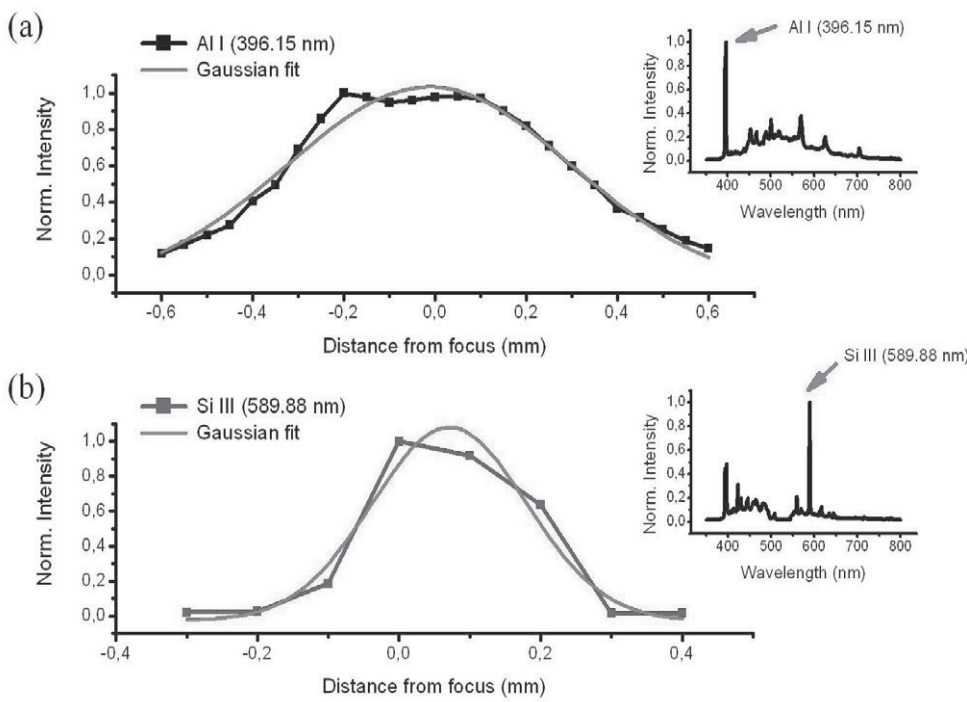

Figure 5. Plasma intensity for different focus distances at a laser wavelength of 1064 nm and pulse width of 20 ns. (a) AlN sample; (b) Borofloat glass sample.

3.4. Thin-layer removal monitoring

The individual lines are scribed in sequence, i.e. in repetitive cycles, and the spectroscopic data is gathered during picosecond laser processing at a wavelength of 532 nm, an energy per pulse of 4 µJ, a XY table speed of 20 mm/s and an integration time of 200 ms for the spectra acquisition. Lines of indium (In I at 451 nm) and molybdenum (Mo I at 379 nm) are identified and the results are shown in Figure 6.

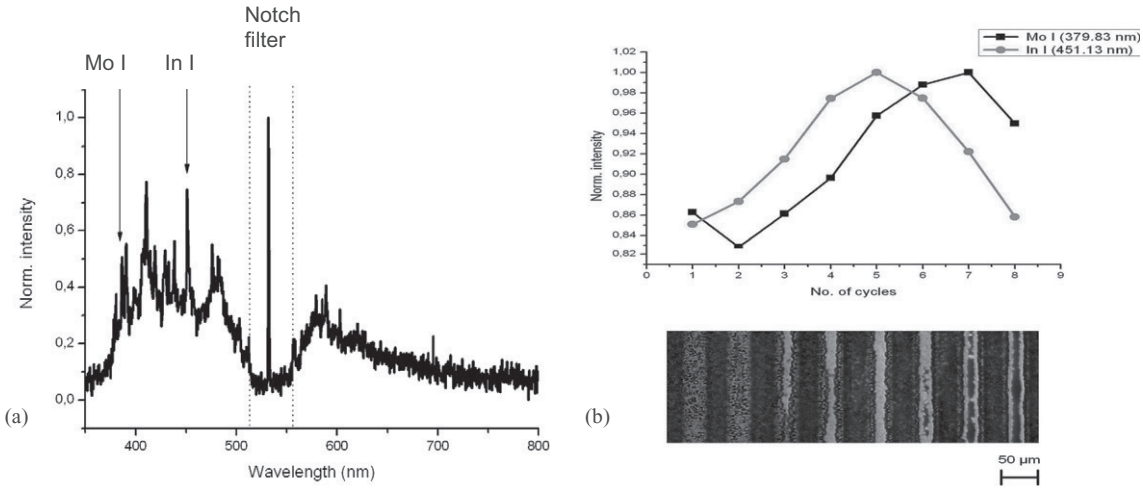

Figure 6. a) Spectrum obtained during solar cell processing. Multiple layers are affected so lines of Mo and In are simultaneously detected; b) Result of scribing an increasing number of lines on top of another and the monitoring of the intensity of specific emission lines during each step.

Laser radiation was mainly absorbed by the CIS film. The laser-induced thermal reaction with plasma formation is observed for the CIS film, while the top ZnO layer is removed in macroscopic fractions. This explains, why Zn signals are not detected in the study. Figure 6a demonstrates that under the outlined experimental conditions, a selective ablation is not obtained over the approx. 5 cycles necessary, to complete the removal of 2 µm CIS on the ca. 0.5 µm Mo layer. The Mo I and In I emission lines are registered simultaneously. However, the maximum intensity in the In I emission line at 451 nm is obtained after the complete 2 µm CIS layer is ablated, see Figure 6b. Two cycles later, the maximum intensity of the Mo I emission line is registered, while the In I line peak has dropped. This cycle number 7 also marked the point, when a major part of the Mo film is removed. These tendencies are reproducible and can be utilized to discriminate the removal threshold and secure a selective removal. Further work is in progress to implement monitoring strategies for selective laser processing of thin films, such as CIS in photovoltaic applications.

4. Conclusions

LIBS has the potential to be used as a monitoring signal for laser machining. Applications, such as material identification and sorting, as well as focus positioning and selective thin-layer removal can be successfully achieved by detecting and analyzing the plasma emission. Identification of correlations in the laser-induced plasma spectra during parameter optimization in the laser (micro) machining process is the decisive goal of the ongoing investigations to outline and implement monitoring strategies in laser machining.

Acknowledgements

Part of this study is supported by the AiF program "Förderung von Vorlaufforschung bei Wachstumsträgern in benachteiligten Regionen" project number VF081026. The authors want to thank the funding of the German Academic Exchange Service (DAAD).

References

[1] Cramers, D.: Handbook of Laser-Induced Breakdown Spectroscopy. John Wiley, 2006
[2] Tong, T.; Li, J.; Longtin, J.P.: Real-time control of ultrafast laser micromachining by laser-induced breakdown spectroscopy. In: Applied Optics 43 (2004), 1971-1980
[3] Gaft, M.; Sapir-Sofer, I.; Modiano, H.; Stana R.: Laser induced breakdown spectroscopy for bulk minerals online analyses. In: Spectrochimica Acta Part B 62 (2007), 1496-1503
[4] Giakoumaki, A.; Melessanaki, K.; Anglos, D.: Laser-induced breakdown spectroscopy (LIBS) in archaeological science—applications and prospects. In: Analytical and Bioanalytical Chemistry 387 (2007), 749-760
[5] Fortes, F.J.; Cabalín, L.M.; Laserna, J.J.: The potential of laser-induced breakdown spectrometry for real time monitoring the laser cleaning of archaeometallurgical objects. In: Spectrochimica Acta Part B 63 (2008), 1191-1197
[6] Lentjes, M.; Dickmann, K.; Meijer, J.: Controlled laser cleaning of artworks with low resolution LIBS and linear correlation analysis. In: ICALEO 2005 Proceedings (2005), 286-292
[7] Balzer, H.; Hoehne, M.; Sturm, V.; Noll, R.: Online coating thickness measurement and depth profiling of zinc coated sheet steel by laser-induced breakdown spectroscopy. In: Spectrochimica Acta Part B 60 (2005), 1172-1178
[8] Mowery, M.D.; Sing, R.; Kirsch, J.; Razaghi, A.; Bechard, S.; Reed, R.A.: Rapid at-line analysis of coating thickness and uniformity on tablets using laser induced breakdown spectroscopy. In: Journal of Pharmaceutical and Biomedical Analysis 28 (2002), 935-943
[9] Schwagmeier, M.; Mueller, N.; Ashkenasi, D.: Laser micro machining of metal foils, ceramics and silicon substrates. In: Proceedings of the Fifth International WLT-Conference on Lasers in Manufacturing (2009)